

An Optimized Method for 3D Magnetic Navigation of Nanoparticles inside Human Arteries

Evangelos G. Karvelas, Christos Liosis, Andreas Theodorakakos, Theodoros E. Karakasidis

Abstract—In the present work, a numerical method for the estimation of the appropriate gradient magnetic fields for optimum driving of the particles into the desired area inside the human body is presented. The proposed method combines Computational Fluid Dynamics (CFD), Discrete Element Method (DEM) and Covariance Matrix Adaptation (CMA) evolution strategy for the magnetic navigation of nanoparticles. It is based on an iteration procedure that intends to eliminate the deviation of the nanoparticles from a desired path. Hence, the gradient magnetic field is constantly adjusted in a suitable way so that the particles' follow as close as possible to a desired trajectory. Using the proposed method, it is obvious that the diameter of particles is crucial parameter for an efficient navigation. In addition, increase of particles' diameter decreases their deviation from the desired path. Moreover, the navigation method can navigate nanoparticles into the desired areas with efficiency approximately 99%.

Keywords—CFD, CMA evolution strategy, DEM, magnetic navigation, spherical particles.

I. INTRODUCTION

MAGNETIC navigation of drugs inside the human arteries is a very important method of drug delivery since it permits to drive the drug to the desired area. Consequently, the quantity of the drug required to reach therapeutic levels is being reduced while the concentration at targeted sites is increased. This concept can be achieved with the use of magnetic nanoparticles where anti-tumor agents are coated on surface. The magnetic field that is required to navigate the particles inside the human arteries can be produced by a Magnetic Resonance Imaging (MRI) device.

The magnetic navigation of drug depends on several parameters [1]-[3]. At first, the materials and the coatings of the particles are significant due to the variety of magnetic properties [4]. The volume of the nanoparticles is a crucial factor for an efficient magnetic navigation of drug. The magnetic response of the small particles seems to be weaker, causing increased adversity for particles to be navigated into arterial system of the human body. For this reason, paramagnetic particles are used which form clusters under the action of permanent magnetic field. These clusters form aggregations that are aligned with the magnetic field lines and

are more responsive to gradient magnetic fields compared to single particles [5]. Advantages of these nanoclusters include enhanced particle uptake in cancer cells with no apparent decrease in the inherent magnetization characteristics, efficient drug loading and tunable cluster size [6]. The magnitude of the imposed permanent magnetic field is a significant parameter since under the action of weak magnitudes, only small aggregations can be formed due to weak dipole interaction forces [7].

In this study, a method for the evaluation of the optimum magnitudes of the gradient magnetic field for three-dimensional navigation of paramagnetic nanoparticles inside a carotid model is presented. In Section II, the numerical procedure for the blood flow, particles' kinetics and simulation details are described. In Section III, results for the influence of diameter of particles in the navigation process are presented. Finally, conclusions are presented in Section IV.

II. NUMERICAL MODEL

A. Governing Equations

In this study a numerical procedure for the evaluation of the optimal gradient magnetic fields for the navigation of magnetic nanoparticles inside a carotid artery is presented. For the propulsion model of the particles, seven major forces are considered, i.e., the magnetic force from MRIs Main Magnet static field as well as the Magnetic field gradient force from the special Propulsion Gradient Coils. The static field is responsible for the aggregation of nanoparticles while the magnetic gradient contributes to the navigation of the agglomerates that are formed. Moreover, the contact forces among the aggregated nanoparticles and the wall, and the Stokes drag force for each particle are considered, while only spherical particles are used in this study. In addition, gravitational forces due to gravity and the force due to buoyancy are included. Finally, Van der Waals force and Brownian motion are taken into account in the simulation. Flow field and the uncoupled equations of particles motion are calculated using the OpenFOAM platform [8]. In addition, a Covariance Matrix Adaptation Evolution Strategy (CMAES) is used in order to verify the optimal gradient magnetic fields and navigate the particles into the desired area. A desired trajectory is inserted into the computational geometry, which the particles are going to be navigated in.

Laminar blood flow is expected to occur in the carotid model. The incompressible Navier–Stokes equations are solved for the Eulerian frame along with a model for the discrete motion of particles in a Lagrangian frame. The governing equations of the fluid phase are given as:

E. G. Karvelas and A. Theodorakakos are with the Mechanical Engineering Department, University of West Attica, Athens, CO 12241 Greece (e-mail: ekarvellas@uniwa.gr, atheod@uniwa.gr).

C. Liosis is with the Civil Engineering Department, University of Thessaly, Volos, CO 38334 Greece (e-mail: cliosis@uth.gr).

T. E. Karakasidis is with the Civil Engineering Department, University of Thessaly, Volos, CO 38334 Greece ((phone: 24710-74163; e-mail: thkarak@civ.uth.gr).

$$\nabla \cdot \mathbf{u} = 0 \quad (1)$$

$$\rho \left(\frac{\partial \mathbf{u}}{\partial t} + \mathbf{u} \cdot \nabla \mathbf{u} \right) = -\nabla p + \mu \nabla^2 \mathbf{u} \quad (2)$$

where t is the time, \mathbf{u} and p are the fluid velocity and pressure, respectively, and ρ and μ are its density and viscosity, respectively. In this study, blood is considered as a non-Newtonian fluid. Therefore, the Bird-Carreau model is adopted, where the viscosity of the blood is given by [9]:

$$\nu = \nu_\infty + (\nu_0 - \nu_\infty) [1 + \lambda^2 \dot{\gamma}^2]^{(n-1)/2} \quad (3)$$

where $\dot{\gamma}$ is the shear rate, ν_∞ is the viscosity at infinite shear rate, ν_0 is the viscosity at zero shear rate, λ relaxation time and n is the power index power.

The equations of every particle single motion in the discrete phase are based on the Newton law and may read as follows:

$$m_i \frac{\partial \mathbf{u}_i}{\partial t} = F_{mag,i} + F_{nc,i} + F_{tc,i} + F_{hydro,i} + F_{boy,i} + W_i + F_{vdw,i} + F_{br,i} \quad (4)$$

$$I_i \frac{\partial \boldsymbol{\omega}_i}{\partial t} = M_{drag,i} + M_{con,i} + T_{mag,i} \quad (5)$$

where the index i stands for the i th-particle with diameter d_i , \mathbf{u}_i and $\boldsymbol{\omega}_i$ are its transversal and rotational velocities, respectively, and m_i is its mass. The mass moment of inertia matrix is I_i , the terms $\frac{\partial \mathbf{u}_i}{\partial t}$ and $\frac{\partial \boldsymbol{\omega}_i}{\partial t}$ correspond to the linear and angular accelerations, respectively. $\mathbf{F}_{mag,i}$ is the total magnetic force, and $\mathbf{F}_{nc,i}$ and $\mathbf{F}_{tc,i}$ are the normal and tangential contact forces, respectively. $\mathbf{F}_{drag,i}$ stands for the hydrodynamic drag force, $\mathbf{F}_{grav,i}$ is the total force due to buoyancy, $\mathbf{M}_{drag,i}$ and $\mathbf{M}_{con,i}$ are the drag and contact moments, respectively, and finally, $\mathbf{T}_{mag,i}$ is the torque due to the magnetic field at the position of particle i .

Details of the numerical models, forces and moments terms used on particles are given in [10]-[12]. For the evaluation of the potential of the computational platform a carotid model is studied here, as depicted in Fig. 1.

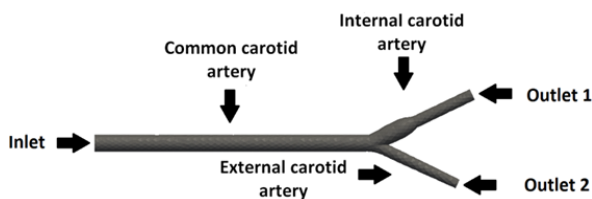


Fig. 1 Carotid Geometry

The dimensions of a human carotid are described in [13]. For the establishment of fully developed velocities profiles before the bifurcation and in order to diminish the numerical issues which are connected to the boundary conditions, the computational geometry is suitably expanded in the inlet and outlets. For this reason, the overall length of the carotid geometry model is 0.3 m. The GMSH generator was used for the 3D computational mesh. Representative view of the

computational unstructured mesh of the carotid is presented in Fig. 2. The computational mesh is consisted of approximately ten thousand triangle elements.

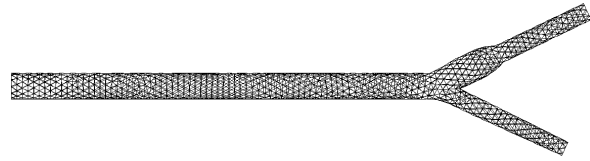


Fig. 2 Computational mesh

B. Determination of the Appropriate Magnetic Gradients

The CMA evolution strategy algorithm [14] is used to navigate the particles into a desired path through successive variations of the magnetic gradient magnitude and sign. The CMA algorithm conducts an iterative principal components analysis of successful search steps, while retaining all principal axes. In addition, two paths of the time evolution of the mean distribution are recorded, called search or evolution paths, respectively. These paths include significant information about the correlation between consecutive steps.

In particular a gradient magnetic field is selected by sampling a multi-variate normal distribution. The basic equation for sampling the gradient magnetic fields, for generation number $g = 0, 1, 2, \dots$ is $x_k^{(g+1)} \sim N(m^{(g)}, (\sigma^{(g)})^2 C^{(g)})$ for $k = 1, \dots, \lambda$, where \sim indicates the same distribution on the left and the right side, $x_k^{(g+1)}$, k th offspring (search point) form generation $g + 1$, $m^{(g)} \in \mathbb{R}^n$, mean value of the search distribution at generation g , $\sigma^{(g)} \in \mathbb{R}^n$, overall standard deviation, step size, at generation g , $C^{(g)} \in \mathbb{R}^n$, covariance matrix at generation g , and $\lambda \geq 2$, population size, sample size, number of offspring.

C. Driving Process

In this work, the above-mentioned method is used for the navigation of paramagnetic nanoparticles in three-dimensional geometries. It should be noted that the present method was successfully used in two-dimensional navigation problems [15]-[17].

The method intends to minimize the particles' position deviation from a desired path. The trajectory in all simulations is pre-described in the computational method by using a 10-degree polynomial as depicted in Fig. 3.

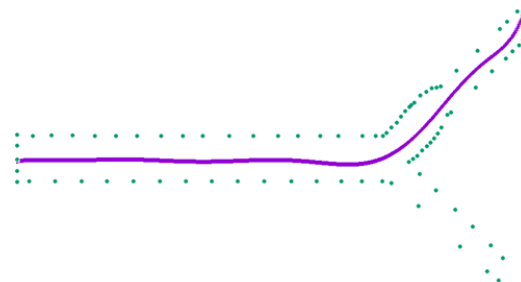


Fig. 3 Desired trajectory (purple line) and boundary of the carotid (green dots)

Initially, blood flow in the carotid, Fig. 1, is achieved by suitably solving (1) and (2). Blood loaded with particles enters the carotid from the left and splits into the two outlet branches at the right side of the domain (Fig. 1). Once the flow and the pressure fields are found, the discrete phase simulation starts with combination of the DEM and the CMA methods. Random magnitudes of the gradient magnetic field are provided from CMA evolution strategy to DEM in the beginning of the process. The DEM method evolves all particles' positions for some time and the deviation between the nanoparticles and the desired path is evaluated in each time step. The CMA algorithm is used in order to minimize this distance by providing better magnitudes of the gradient magnetic field in a way to eliminate the deviation of the nanoparticles from the desired path. Hence, the appropriate magnitudes of the gradient magnetic field are evaluated for optimum navigation of nanoparticles into the desired area. Representative duration of the numerical simulation under 18 variations of the gradient magnetic field is 24 h of CPU time on a cluster with 24 Intel Xenon CPUs (2.4 Ghz) and 128 Gb of memory.

D. Simulation Details

In this study, particles from 200 nm to 900 nm are used for the evaluation of the computational method. One thousand Fe_3O_4 spherical particles are used in each simulation with concentration equal to 10 mg/ml. Parameters of the simulated particles are presented in Table I.

TABLE I
 PROPERTIES OF THE SIMULATED PARTICLES

Symbol	Quantity	SI
ρ	particles density	5000 Kg/m ³
E	Young's modulus	3.5×10 ⁹ Pa
ν	Poisson's ratio	0.34
μ_r	Particles rel. mag. permeability	1.23
μ	Permeability of medium	1.25×10 ⁻⁶
T	Temperature	288 K
λ	Molecular mean free path	2.5×10 ⁻⁹

TABLE II
 BOUNDARY CONDITIONS

Boundary	Velocity	Pressure
Inlet	0.08m/s	Zero gradient
Outlet 1	Zero gradient	0
Outlet 2	Zero gradient	0
Walls	0	Zero gradient

In present study, we intend to navigate the nanoparticles under the combined action of permanent and gradient magnetic fields from the common to the internal carotid artery (Fig. 1). Therefore, the desired trajectory (Fig. 3) is successfully transformed in order to be described as a 10-degree polynomial and imported in the computational platform. It should be noted that the steady magnetic field magnetic field is set equal to $B_0 = 10$ T while the magnetic gradient is constantly changing in order to drive the nanoparticles as close in the desired path. It should be noted that the magnetic gradient is changing 18 times in each

simulation. In addition, each iteration of the computational method includes 1000 evaluations of the gradient magnetic field values. The boundary conditions that were used for the evaluation of the fluid flow are given in Table II.

III. RESULTS

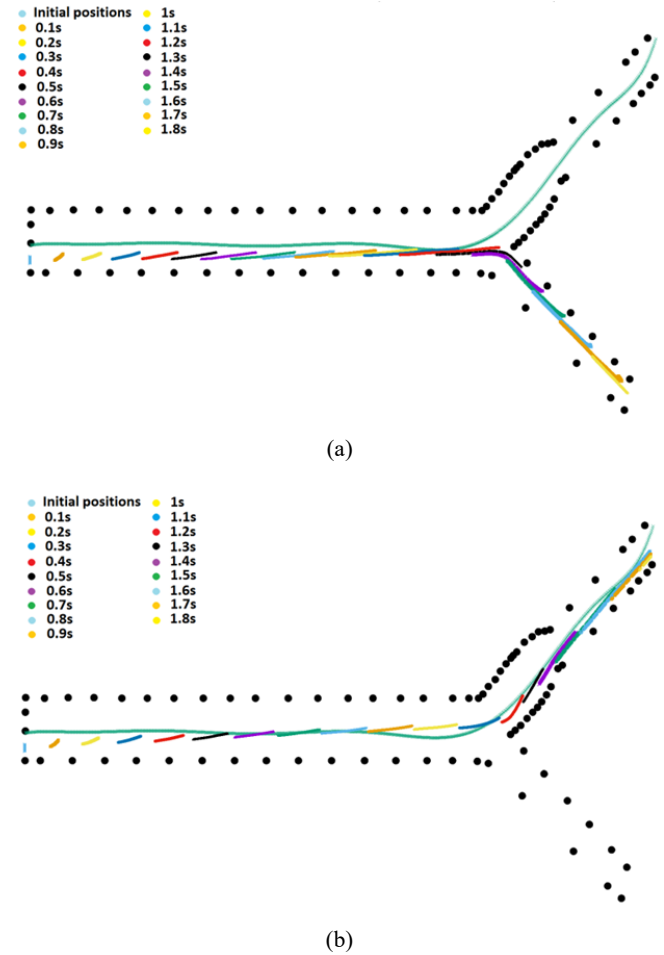
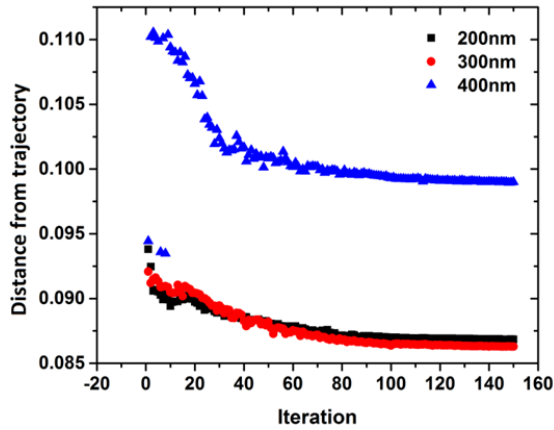


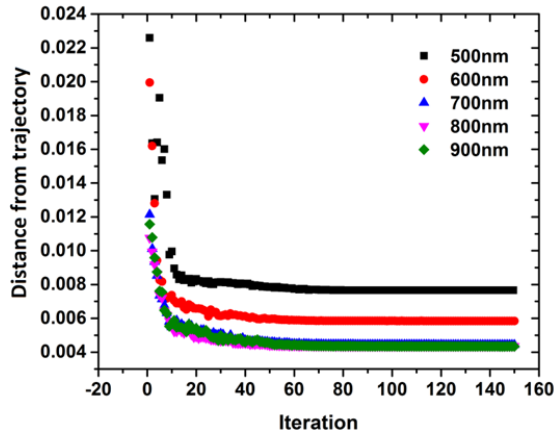
Fig. 4 Projection of the positions of particles under different time steps of the navigation process for particles with diameter of (a) 200 nm and (b) 500 nm

In the present study, the computational method is used in order to navigate the nanoparticles from the common to the internal carotid artery through a desired trajectory (Figs. 1, 3). The particles follow the stream lines of the blood flow while they undergo 18 variations of the gradient magnetic field in order to follow as close as possible the desired trajectory. The diameter of the particles is a crucial parameter for an effective magnetic navigation. The magnetic moment of the particles is strongly connected with the volume of the particles. Therefore, particles with small diameters are very difficult to navigate towards the desired locations. This effect is depicted in Fig. 4 where the particles with diameter of 200 nm are not navigated into the desired branch of the carotid (Fig. 4 (a)). It should be noted that the computational platform under the permitted limits of the imposed gradient magnetic fields are not able to successfully navigate the particles. On the other

hand, under the same magnetic gradient limits and under gradient magnetic field adjustments, the particles with diameter of 500 nm are following as close as possible the desired trajectory, as is depicted in Fig. 4 (b).

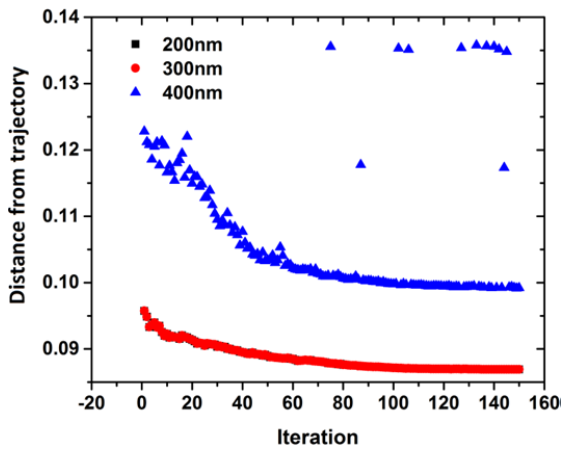


(a)

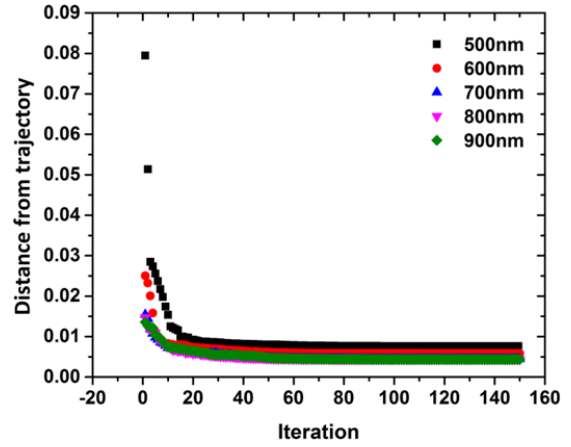


(b)

Fig. 5 Best distance of particles in each iteration from the desired trajectory for (a) particles 200-400 nm and (b) particles 500-900 nm

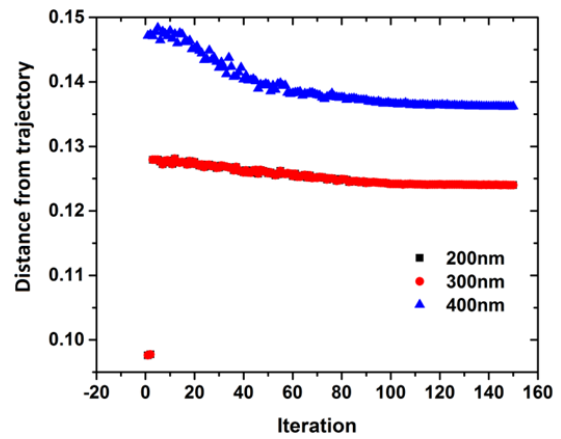


(a)

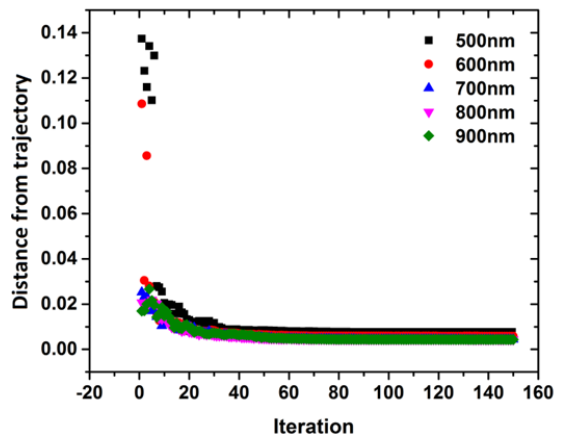


(b)

Fig. 6 Median distance of particles in each iteration from the desired trajectory for (a) particles 200-400 nm and (b) particles 500-900 nm



(a)



(b)

Fig. 7 Worst distance of particles in each iteration from the desired trajectory for (a) particles 200-400 nm and (b) particles 500-900 nm

Results of the present study indicate that particles with diameter from 200 nm to 400 nm under the imposed gradient limits are unable to be navigated into the desired location. On the other hand, the computational platform can successfully

navigate particles with diameter above 500 nm.

The closer (best), median and worst distances of nanoparticles from the pre-described trajectory in the whole simulation and in each iteration of the computational model for the whole range of the simulated diameters are depicted in Figs. 5, 6 and 7, respectively. It should be pointed out that the evolution of the simulation process leads the elimination of the distances of nanoparticles from the desired path in each iteration. Therefore, the computational platform performs validation and selects the best values of the gradient magnetic field for optimum magnetic driving of nanoparticles, as depicted in Fig. 5. Since its iteration is composed by 1000 evaluations of different gradient magnetic fields, the evolution of median and worst distance of nanoparticles from the desired path is depicted in Figs. 6 and 7.

Results indicate that diameter of particles plays a significant role since in the range of 200-400 nm the magnetic field is not sufficient enough in order to move the particles close to the desired trajectory (Fig. 5 (a)) and therefore the distances are higher than that of particles in the range of 500-900 nm (Fig. 5 (b)).

From Figs. 5-7 it is clear that the computational platform can evaluate and detect the appropriate values of the gradient magnetic field in the particles follow the desired trajectory in only 10 iterations. The rest of the iterations are performed in order to navigate the particles as close in the desired trajectory.

IV. CONCLUSIONS

The proposed model can simulate the motion of nanoparticles in the magnetic navigation process in a carotid model. Under the influence of the blood flow the model evaluates the effect of different magnitudes of the gradient magnetic field in order to minimize the deviation of nanoparticles from a pre-described trajectory. Moreover, the platform can navigate the nanoparticles into the desired path with an efficiency of approximately 99%. The computational time that is needed for a successful evaluation of the appropriate magnitudes of the gradient magnetic field for navigation of nanoparticles in the desired branch of the carotid is approximately 2 hours while approximately another 22 hours are needed for optimum magnetic navigation as close to the desired trajectory. The diameter of particles is a crucial parameter for an effective magnetic navigation. Therefore, for an efficient navigation of small particles the magnitudes of the permanent and gradient magnetic field should be increased.

ACKNOWLEDGMENT

This research is co-financed by Greece and the European Union (European Social Fund- ESF) through the Operational Programme "Human Resources Development, Education and Lifelong Learning 2014-2020" in the context of the project "Magnetic driving of nanoparticles in human arteries' networks" (MIS: 5048923).

REFERENCES

- [1] Q. Pankhurst, J. Connolly, S. Jones, J. Dobson, Applications of magnetic nanoparticles in biomedicine, *J. Phys. D: Appl. Phys.*, vol. 36, no. 13, pp. 167–181, 2003.
- [2] M. Ramezani, S.S.W. Leung, K.H. Delgado-Magnero, B.Y.M. Bashe, J. Thewalt, D.P. Tieleman, Computational and experimental approaches for investigating nanoparticle-based drug delivery systems, *Biochim. Biophys. Acta*, vol. 1858, pp. 1688–1709, 2016.
- [3] V.P. Podduturi, I.B. Magana, D.P. O'Neal, P.A. Derosa, Simulation of transport and extravasation of nanoparticles in tumors which exhibit enhanced permeability and retention effect, *Comput. Methods Programs Biomed.*, vol. 112, pp. 58–68, 2013.
- [4] J. Llandro, J.J. Palfreyman, A. Ionescu, C.H.W. Barnes, Magnetic biosensor technologies for medical applications: a review, *Med. Biol. Eng. Comput.*, vol. 48, pp. 977–998, 2010.
- [5] P. Babinec, A. Krafcik, M. Babincova, J. Rosenecker, Dynamics of magnetic particles in cylindrical halbach array: implications for magnetic cell separation and drug targeting, *Med. Biol. Eng. Comput.*, vol. 48, pp. 745–753, 2010.
- [6] D.H. Nguyen, J.S. Lee, J.H. Choi, K.M. Park, Y. Lee, K.D. Park, Hierarchical self-assembly of magnetic nanoclusters for theranostics: tunable size, enhanced magnetic resonance imaging, and controlled and targeted drug delivery, *Acta Biomaterialia*, vol. 35, pp. 109–117, 2016.
- [7] K. Widder, P. Marino, R. Morris, A. Senyei, *Targeted Drugs*, Wiley, New York, 1983.
- [8] H.G. Weller, G. Tabor, H. Jasak, C. Fureby, A tensorial approach to computational continuum mechanics using object-oriented techniques, *Comput. Phys.*, vol. 12, no. 6, pp. 620–631, 2010.
- [9] P. Kennedy and R. Zheng, *Flow Analysis of Injection Molds*: Hanser, 2013.
- [10] E.G. Karvelas, N.K. Lampropoulos, I.E. Sarris, A numerical model for aggregations formation and magnetic driving of spherical particles based on OpenFOAM, *Comp. Methods Progr. Biomed.*, vol. 142, pp. 21–30, 2017.
- [11] E.G. Karvelas, T.E. Karakasidis, I.E. Sarris, Computational analysis of paramagnetic spherical Fe_3O_4 nanoparticles under permanent magnetic fields, *Comput. Mat. Sci.*, vol. 154, pp. 464–471, 2018.
- [12] E.G. Karvelas, N.K. Lampropoulos, L. Benos, T.E. Karakasidis, I.E. Sarris, On the magnetic aggregation of Fe_3O_4 nanoparticles, *Comp. Methods Progr. Biomed.*, DOI: 10.1016/j.cmpb.2020.105778
- [13] B.K. Bharadvaj, R.F. Mabon, D.P. Giddens, Steady flow in a model of a human carotid bifurcation. part 1-Flow visualization. *J. Biomech.* vol. 15, pp. 349–362, 1982.
- [14] N. Hansen, The CMA evolution strategy; a comparing review, *Adv. Estim. Distrib. Algorithms*, vol. 192, pp. 1769–1776, 2006.
- [15] N.K. Lampropoulos, E.G. Karvelas, D.I. Papadimitriou, I.E. Sarris, Computational study of the optimum gradient magnetic field for the navigation of spherical particles into targeted areas, *Journal of Physics: Conference Series* vol. 637, no. 1, pp. 012038, 2015.
- [16] N.K. Lampropoulos, E.G. Karvelas, T.E. Karakasidis, I.E. Sarris, Computational Study of the Optimum Gradient Magnetic Field for the Navigation of the Spherical Particles in the Process of Cleaning the Water from Heavy Metals, *Procedia Engineering*, vol. 162, pp. 77–82, 2016.
- [17] N.K. Lampropoulos, E.G. Karvelas, D.I. Papadimitriou, T.E. Karakasidis, I.E. Sarris, Computational study of the effect of gradient magnetic field in navigation of spherical particles, *Journal of Physics: Conference Series*, vol. 931, no. 1, pp. 012014, 2017.